

## Interactions between trophoblast and uterine epithelium: monitoring of adhesive forces

Michael Thie<sup>1,3</sup>, René Röspe<sup>1</sup>, Wolfgang Dettmann<sup>2</sup>,  
Martin Benoit<sup>2</sup>, Markus Ludwig<sup>2</sup>,  
Hermann E.Gaub<sup>2</sup> and Hans-Werner Denker<sup>1</sup>

<sup>1</sup>Institut für Anatomie, Universitätsklinikum, Hufelandstraße 55, D-45122 Essen and <sup>2</sup>Lehrstuhl für Angewandte Physik, Ludwig-Maximilians-Universität, Amalienstraße 54, D-80799 München, Germany

<sup>3</sup>To whom correspondence should be addressed

At embryo implantation, it is postulated that the initial contact between blastocyst and maternal tissues is by adhesion of the trophoblast to the uterine epithelium. This cell-to-cell interaction is thought to be critical for implantation, although the actual adhesive forces have never been determined. In the present study, the atomic force microscope (AFM) was used to study the adhesion between human uterine epithelial cell lines (HEC-1-A; RL95-2) and human trophoblast-type cells (JAR). Specific interaction forces of these epithelia via their apical cell poles were determined on the basis of approach-and-separation cycles. For this purpose, the AFM tip was functionalized with JAR cells, then brought to the surface of uterine epithelial monolayers and was kept in contact for different periods of time (ms, 1, 10, 20, 40 min). The approach force curves displayed repulsive interactions for both HEC-1-A and RL95-2 cells. However, RL95-2 cells (with a smooth surface structure and a thin glycocalyx) showed lower values of the repulsive regime than HEC-1-A cells (with a rough surface structure and a thick glycocalyx). After having overcome repulsive interactions, the initial contact was followed by adhesive interactions. For contact times of 20 and 40 min, RL95-2 cells, but not HEC-1-A cells, showed specific JAR binding, i.e. the separation force curves displayed repeated rupture events in the range of 1–3 nN with a distance between 7–15 µm and, thereafter, a final rupture event at a distance of up to 45 µm. These features point to the formation of strong cell-to-cell bonds. Collectively, these studies provide the first definition of interaction forces between the trophoblast and the uterine epithelium, and are consistent with the hypothesis that an RL95-2-like architecture of uterine epithelial cells, i.e. an non-polarized phenotype, is essential for apical adhesiveness for the human trophoblast.

**Key words:** adhesion force/atomic force microscope/trophoblast/uterine epithelium

### Introduction

Embryo implantation is a complex process that is initiated, in all species, by an interaction of the trophoblast with epithelial cells lining the uterine wall. This interaction is generally assumed to involve cell-to-cell adhesion between these two different epithelia, although the actual adhesive forces have never been determined so that even the whole concept has recently been questioned (Lopata, 1996). In invasive types of implantation, as in the human (Lindenberg *et al.*, 1986), adhesion is followed by penetration of the trophoblast through the uterine epithelium and arrosion of maternal blood vessels (for recent reviews, see Rogers, 1995; Tabibzadeh and Babaknia, 1995; Lopata, 1996). Critical for the whole process (and common to all modes of implantation) appears to be the adhesive interaction between the two epithelia, the trophoblast and the uterine epithelium (for review, see Denker, 1993). With respect to the uterine epithelium, this interaction seems to be possible only in a specific state called receptivity which is hormonally controlled (Psychoyos, 1995). The adhesive properties of the apical surface of uterine cells might be facilitated by changes in the structural organization of the apical cell pole. It has been proposed that part of a master gene programme for the epithelial phenotype, including genes for apical–basal polarity, may be turned off and, vice versa, certain genes for the mesenchymal programme may be turned on, at this particular state (Denker, 1994; Thie *et al.*, 1996a).

The molecular steps leading to the development of adhesiveness of human uterine epithelial cells cannot be investigated *in vivo*, and problems with *in-vitro* explants of receptive uterine tissue have not been solved satisfactorily (e.g. Carson *et al.*, 1988; Glasser *et al.*, 1988; Bentin-Ley *et al.*, 1994). Thus, the role of epithelial cells in human implantation has largely been studied in model experiments using endometrial cell lines (e.g. Raboudi *et al.*, 1992; John *et al.*, 1993; Rohde and Carson, 1993; Thie *et al.*, 1995; Rohde *et al.*, 1996; Thie *et al.*, 1996b). Among them, HEC-1-A (Kuramoto *et al.*, 1972) and RL95-2 cells (Way *et al.*, 1983) appear to be useful models to investigate features of apical adhesiveness of uterine epithelial cell phenotypes. RL95-2 cells do, but HEC-1-A cells do not allow trophoblast-type cells to attach at their apical pole (John *et al.*, 1993). Nevertheless, both cell lines have been shown to possess the same sets of adhesion molecules and cytoskeletal proteins, but they differ with respect to their organization along the apico-basal axis (Thie *et al.*, 1995, 1996b).

The purpose of the present study was to provide quantitative data on the adhesive forces measurable at the apical (free) pole of the cells, using a novel type of application of the atomic force microscope (Binnig *et al.*, 1986; Rugar and Hansma, 1990; Radmacher *et al.*, 1992). Specifically, human trophoblast-type (JAR) cells (Pattillo *et al.*, 1971) were brought into contact with monolayers of HEC-1-A and RL95-2 cells via the apical plasma membrane domain for various periods of time. Forces were measured first while lowering the JAR cells on to the free surface of endometrial cells. Forces were then continuously recorded during several cycles of approach and separation. It was thus possible to identify and measure repulsive forces exerted during the initial contact, followed by adhesive interactions developing slowly thereafter. Our observation that there are distinct rupture events upon separation of RL95-2 and JAR cells, but not upon separation of HEC-1-A and JAR cells, indicates specific features of cell-to-cell bonds between RL95-2 (but not HEC-1-A) and JAR cells. Results are interpreted in terms of current models of the behaviour of uterine epithelial cells during embryo adhesion.

## Materials and methods

### Routine cell culture

Human endometrial cell lines were purchased from the American Type Culture Collection (ATCC), Rockville, MD, USA, i.e. HEC-1-A cells (HTB 112; Kuramoto *et al.*, 1972) and RL95-2 cells (CRL 1671; Way *et al.*, 1983). For routine culture, cell lines were grown in plastic flasks in 5% CO<sub>2</sub>-95% air at 37°C. In brief, HEC-1-A cells were seeded out in McCoy's 5A medium (Gibco-Life Technology, Eggenstein, Germany) supplemented with 10% fetal calf serum (Gibco), RL95-2 cells in a 1 + 1 mixture of Dulbecco's modification of Eagle's medium and Ham's F12 (Gibco) supplemented with 10% fetal calf serum, 10 mM HEPES (Gibco), and 0.5 µg/ml insulin (Gibco). All media were additionally supplemented with penicillin (100 IU/ml; Gibco) and streptomycin (100 µg/ml; Gibco). The growth medium was changed every 2 to 3 days, and cells were subcultured by trypsinization (trypsin-EDTA solution; Gibco) when they became confluent.

### Preparation of microbead-mounted cantilever

Long-legged cantilevers (DNP-S cantilever; Digital Instruments, Santa Barbara, CA, USA) with a spring constant of 50 mN/m were used. A tiny spot of glue (UHU plus endfest 300, Bühl, Germany) was applied to the tip of a cantilever using glass electrodes normally prepared for the patch clamp technique. Then a single Sephacryl S-1000-bead (80 ± 20 µm in diameter; Pharmacia, Freiburg, Germany) sticking electrostatically to a cannula (Terumo no. 20, Leuven, Belgium) was placed on the glue. In order to harden the glue, the microbead-mounted cantilever was then heated at 75°C for 45 min followed by 22°C for 12 h. Before use, cantilevers were sterilized in 70% ethanol for 2 h, and washed thoroughly in distilled water.

### Cell culture on cantilever

Cantilevers mounted with microbeads as described above were immersed in 0.01% poly-D-lysine for 1 h at room temperature, washed in medium for several times, and subsequently incubated with a human JAR choriocarcinoma cell suspension (ATCC: HTB 144; Pattillo *et al.*, 1971) (2 × 10<sup>5</sup> cells per ml RPMI 1640 medium, Gibco, supplemented with 10% fetal calf serum and 0.1% glutamine). After the JAR cells had settled, these cantilever-cell combinations

were incubated as described above. Usually 3 to 4 days after the start of cultures, cells were grown to confluency and cantilevers were now ready to be used for experiments.

For control experiments, microbead-mounted cantilevers were coated with bovine serum albumin (BSA) (Cohn V Fractionate, A 8022; Sigma-Aldrich, Deisenhofen, Germany) by adsorption. For this purpose, microbead-mounted cantilevers were immersed in a 25 µg/ml BSA solution. After 1 h at 20°C the cantilevers were transferred to JAR medium (see above) and subsequently used for experiments.

### Measurement of binding forces

A custom-made atomic force microscope (Florin *et al.*, 1994; Ludwig *et al.*, 1997; Rief *et al.*, 1997) with a vertical range of 100 µm at 16-bit resolution and microbead-mounted cantilevers (see above) were used for the experiments. All experiments were performed in a liquid environment, i.e. JAR medium. Thus, the medium of the confluent endometrial monolayers (see above) was replaced with RPMI 1640 medium supplemented with 10% fetal calf serum and 0.1% glutamine prior to experiments. At given culture conditions (28°C; pH 7.5), forces between the microbead and the confluent endometrial monolayers were measured by cantilever deflection during the approach and the separation of the cantilever (Florin *et al.*, 1994; Dammer *et al.*, 1995; Hinterdorfer *et al.*, 1996; Ludwig *et al.*, 1997; Rief *et al.*, 1997). In brief, the approach force curve was measured while the microbead-mounted cantilever was brought into contact with the surface of endometrial monolayers at a rate of 6.8 µm/s. Upon reaching an indentation threshold force of 2.6 nN, which corresponds to a pressure of 5.2 pN/µm<sup>2</sup> acting on a contact area of 500 µm<sup>2</sup>, the approach was stopped. This contact was kept for variable periods of time (ms, 1, 10, 20, 40 min). The adhesion force curve was measured while the cantilever was separated from the sample at a pulling rate of 6.8 µm/s. In the case of long contact times, the reflection of the detecting beam was disturbed due to thermal drift and density fluctuations of the living cells on the cantilever. This affects the constant deflection feedback loop and leads to fluctuations of loading forces. Experiments were repeated five (BSA-coated microbeads) and 15 times (JAR-coated microbeads), respectively. Each cantilever was used for only one experiment. Data analysis was performed on a MacIntosh Power PC using Igor Pro software. The elastic properties of the cells (i.e. the Young-Modulus) were estimated with the Hertz model (Hertz, 1881; Radmacher *et al.*, 1995).

### Electron microscopy

Endometrial cells were grown on poly-D-lysine-coated thermanox coverslips (Nunc, Napperville, IL, USA) to confluency. Trophoblastic cells were grown on microbeads mounted on cantilevers. For subsequent scanning electron microscopy (SEM), samples were fixed in 2.5% glutardialdehyde in 0.1 M cacodylate buffer, pH 7.4, for 30 min at room temperature. After repeated washings in distilled water, samples were dehydrated with ethanol, and critical point dried using methanol as intermedium and carbon dioxide as drying medium. Then samples were sputtered with a conductive layer of gold and imaged with a Philips SEM 515. For transmission electron microscopy (TEM), endometrial cells were rinsed twice in phosphate-buffered saline and fixed in 2.5% glutardialdehyde in 0.1 M cacodylate buffer, pH 7.4, for 30 min at room temperature, washed in cacodylate buffer, post-fixed with 1% OsO<sub>4</sub> in cacodylate buffer, dehydrated with ethanol and propylene oxide and embedded in epoxy resin (Cross, 1989). The embedded cells were separated from the thermanox coverslip by snap freezing in liquid nitrogen. Ultrathin sections were

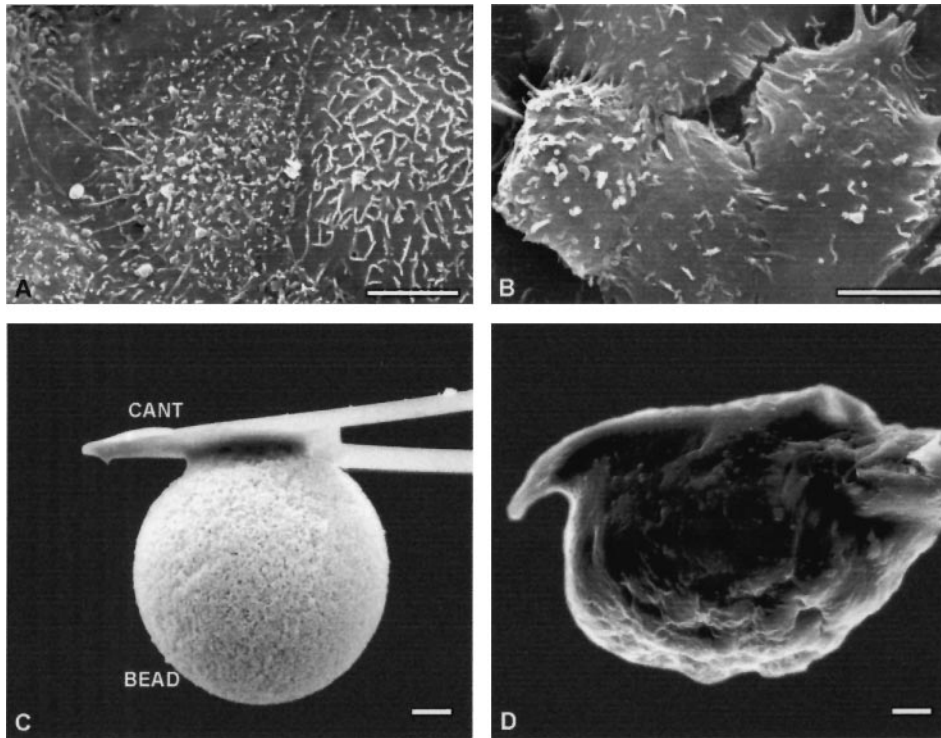


**Figure 1.** Human uterine epithelial monolayers (A, B) and microbead-mounted cantilevers (C, D) imaged by scanning electron microscopy. The free surface of HEC-1-A cells appears to be rough and numerous microvilli and microridges cover the cells (A). In contrast, the free surface of RL95-2 appears to be rather smooth and microvilli are rare (B). The microbeads (BEAD), glued to the cantilevers (CANT) were coated either with bovine serum albumin (25  $\mu\text{g}/\text{ml}$ ) (C) or with human trophoblast-type JAR cells (D). Scale bars = 5  $\mu\text{m}$  (A, B), 10  $\mu\text{m}$  (C, D).

mounted on 200-mesh copper grids, double-stained with uranyl acetate and lead citrate and examined with a Zeiss EM 902A.

## Results

### General morphology

Measurements to calculate the surface forces were performed on HEC-1-A (HEC cells) and RL95-2 (RL cells). Using transmission electron microscopy, the ultrastructure of HEC cells and RL cells was found to be essentially the same, under the culture conditions used, as described previously (Thie *et al.*, 1995). According to this, HEC cells showed an apical-basal polarized phenotype, while RL cells lacked apical-basal polarity. Scanning electron microscopy was used to illustrate the surfaces of these endometrial cell lines. In particular, the apical (free) surface of HEC cells exhibited a dense lawn of microvilli and microridges (Figure 1A), whereas the apical membrane of RL cells was rather smooth (Figure 1B).

The data reported refer to approach and separation between the free surface of confluent monolayers and that of the opposed probe, i.e. the microbead-mounted cantilever. As a standard, a microbead coated with BSA by adsorption from a 25  $\mu\text{g}/\text{ml}$  BSA solution was used (Figure 1C). Then, a microbead coated with trophoblast-type JAR cells was applied as a functionalized sensor. JAR cells were located on the microbead, forming a confluent layer as shown by scanning electron microscopy (Figure 1D).

Forces between the microbead-mounted cantilever and the endometrial monolayer were measured by cantilever deflection

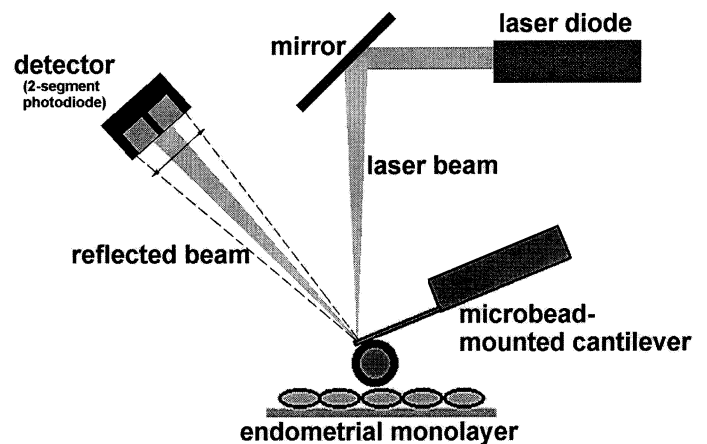


**Figure 2.** Schematic of atomic force microscope operation showing the microbead-mounted cantilever in contact with the endometrial monolayer. Cantilever deflection is measured by a laser beam as indicated.

during the approach and the separation of the cantilever as shown in Figure 2.

### Force measurements with BSA-coated microbeads

Repulsive forces recorded with BSA-coated microbeads (BSA-beads) are illustrated in Figure 3A, B for the approach part of the measuring cycle. While the data reported are derived from all curves in general, typical force curves are given for demonstration. Force versus distance curves displayed a characteristic pattern that allowed us to discern and to define

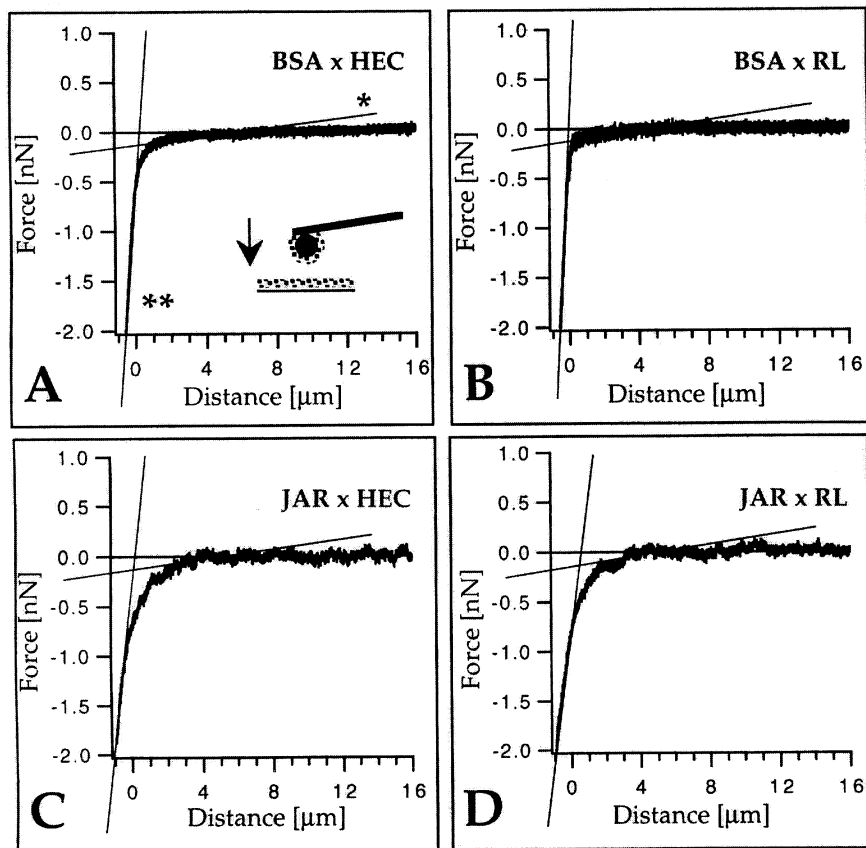


**Figure 3.** Typical repulsive force curves for HEC-1-A and RL95-2 cells during approach cycles recorded with either a bovine serum albumin (BSA)-coated microbead (BSA) (A, B) or a JAR-coated microbead (JAR) (C, D). The horizontal axis shows the vertical movement of the cantilever; the vertical axis shows the force acting on the microbead. The tangent line with the slight slope (Young's-modulus smaller than 10 Pa) (\*) indicates the soft repulsion regime, and the tangent line with the steep slope (Young's-modulus greater than  $10^3$  Pa) (\*\*) indicates the hard repulsion regime.

BSA×HEC = interactions between a BSA-coated microbead and a HEC-1-A monolayer; BSA×RL = interactions between a BSA-coated microbead and a RL95-2 monolayer; JAR×HEC = interactions between a JAR-coated microbead and a HEC-1-A monolayer; JAR×RL = interactions between a JAR-coated microbead and a RL95-2 monolayer.

two distinct types of repulsive interaction: long-ranged soft repulsion (Young's-modulus  $<10$  Pa), followed by hard repulsion (Young's-modulus  $>10^3$  Pa). HEC cells showed soft repulsion as far out as  $2.6 \pm 0.4$   $\mu\text{m}$ . The hard repulsion started at an indentation force of approximately  $0.8 \pm 0.2$  nN after a continuous transition. RL cells showed soft repulsion in a range similar to that of the HEC cells. However, the transition from soft to hard repulsion was abrupt and started at lower indentation forces ( $0.4 \pm 0.2$  nN).

With respect to the subsequent retraction part of the measuring cycle, typical force versus distance curves showing the adhesive forces between a BSA bead and the surface of HEC or RL monolayers are given in Figure 4A, B and Figure 5A, B. During separation, the first part of the curve reflected the reversal of the previous indentation of the bead into the cell monolayer, which decreased with retraction until the point of zero applied force to the cantilever (i.e. zero-force point) was reached. In the case of adhesive interaction, there was a transition from the repulsive to the adhesive regime (i.e. the cantilever was now bent into the opposite direction, while the distance increased). As can be seen, the magnitude of the adhesion forces and the distance at which the surfaces finally separated completely depended on the duration of the

contact. When retraction was started within milliseconds after initial contact (Figure 4A, B) the maximum adhesion was found to be  $0.4 \pm 0.1$  nN on HEC cells and slightly lower ( $0.2 \pm 0.1$  nN) on RL cells. In each case, the surfaces separated at a distance of 2–3  $\mu\text{m}$  from the zero-force point. When the microbead was brought into contact for a longer time (Figure 5A, B), the measured maximum adhesion increased considerably for both HEC and RL monolayers. The measured maximum adhesive forces pointed to saturation when contact times exceeded 20 min (not shown). The adhesive maximum observed with HEC cells after prolonged contact ranged from  $25 \pm 7$  nN at distances of 3–15  $\mu\text{m}$  above the zero-force point. In the case of RL cells,  $30 \pm 10$  nN at distances of 2–15  $\mu\text{m}$  were measured. A sharp adhesion peak followed by a smooth shoulder with increasing distance was characteristic for both cell types. The width of the curves measured at the half adhesion maximum was 8–20  $\mu\text{m}$  for HEC and for RL cells.

#### Force measurements with JAR-coated microbeads

Data on repulsive forces recorded during the approach phase of JAR-coated microbeads (JAR-beads) against HEC or RL monolayers are shown in Figure 3C, D. Typical force curves are given here for demonstration, while the data reported are

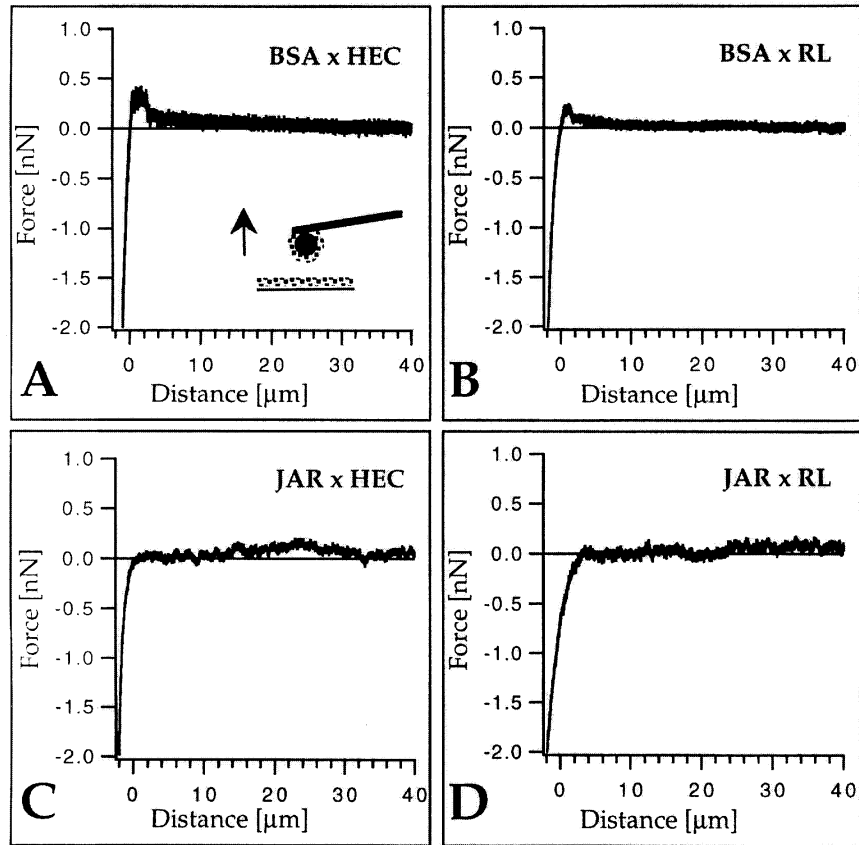


**Figure 4.** Typical adhesive force curves for HEC-1-A and RL95-2 cells resulting when a bovine serum albumin (BSA)-coated microbead (BSA) (**A**, **B**) or a JAR-coated microbead (JAR) (**C**, **D**) was retracted within milliseconds after initial contact. The horizontal axis shows the vertical movement of the cantilever; the vertical axis shows the force acting on the microbead. Note that only BSA-microbeads showed immediate adhesion while JAR-covered microbeads did not. For interaction code see Figure 3.

derived from the total of all curves obtained. As in the case of BSA-beads, the approach of JAR-beads displayed long-range soft repulsion followed by hard repulsion. The transition from the soft repulsion regime to the hard repulsion regime was continuous for both cell types. In contrast to the BSA-beads, JAR-beads showed soft repulsion for a longer distance range, i.e.  $4.0 \pm 0.3 \mu\text{m}$  in HEC cells and  $3.4 \pm 0.4 \mu\text{m}$  in RL cells. The hard repulsion started at higher indentation forces, i.e.  $1.0 \pm 0.2 \text{ nN}$  in HEC cells and  $0.7 \pm 0.2 \text{ nN}$  in RL cells.

Typical force versus distance curves showing the adhesive forces between JAR-beads and the surface of HEC or RL monolayers are given in Figure 4C, D and Figure 5C, D. When JAR-beads were separated from the monolayers within milliseconds after contact, no adhesion was observed (Figure 4C, D), which was in contrast to the measurable (although low) adhesion of the BSA-beads (Figure 4A, B). However, considerable adhesive forces were measured when the duration of contact was increased (Figure 5C, D). One minute after initial cell-to-cell contact, the adhesive maximum was  $7.1 \pm 2 \text{ nN}$  on HEC cells and  $4.2 \pm 2 \text{ nN}$  on RL cells. In each of these cases, JAR and RL/HEC cell surfaces separated completely at a distance of about  $30\text{--}33 \mu\text{m}$  from the zero-force point. With contact times of 1 min, profiles of separation curves were similar for HEC cells and RL cells, i.e. the separation curves showed a sharp peak and a smooth shoulder

with increasing distance. The width of the curve measured at the half adhesion maximum was  $5\text{--}8 \mu\text{m}$  on HEC cells and  $7\text{--}12 \mu\text{m}$  on RL cells.

However, when the JAR-bead was brought into contact for a prolonged time, i.e. 20 or 40 min, the force versus distance curves showed marked differences between HEC (Figure 5C) and RL cells (Figure 5D). HEC cell separation curves were characterized by a sharp peak at a distance of  $4\text{--}5 \mu\text{m}$  from the zero-force point and a smooth shoulder with increasing distance, quite comparable to shorter contact time findings. HEC cell adhesive maxima were about  $16 \pm 4 \text{ nN}$  and peak widths at half adhesion maximum measured  $8\text{--}20 \mu\text{m}$ . RL cells, in contrast, showed force versus distance curves characterized by a broad peak at a distance of  $5\text{--}45 \mu\text{m}$  from the zero-force point, exhibiting discrete force rupture events with increasing distance. Unlike all other systems, the adhesion forces of RL cells did not decrease continuously with increasing distance but exhibited discontinuous force jumps of  $1\text{--}3 \text{ nN}$  with  $7\text{--}15 \mu\text{m}$  distance in between. The final contact ruptured at forces of  $15 \pm 4 \text{ nN}$ . The width of the broadened peak ranged up to  $45 \mu\text{m}$ .

## Discussion

In this study, we report actual measurements of the repulsive and adhesive forces between two epithelia. Using a modified

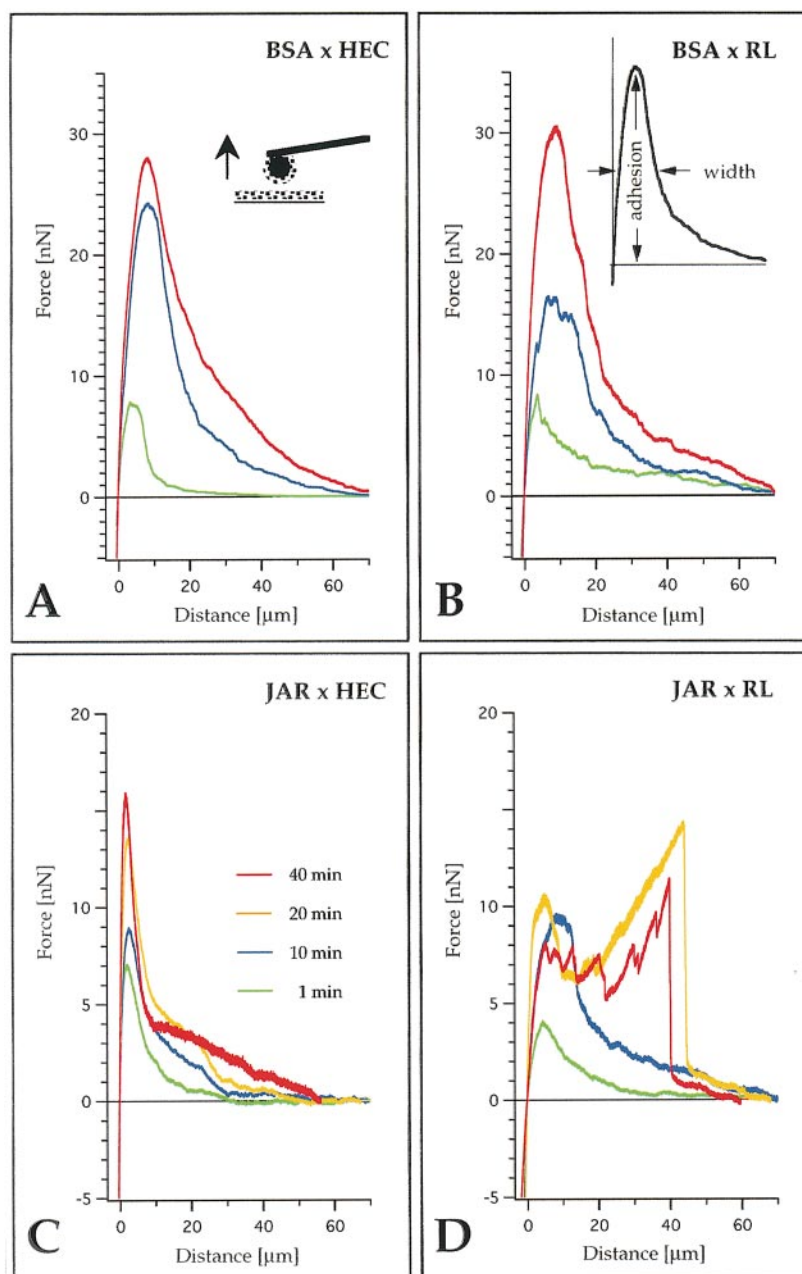


**Figure 5.** Typical adhesive force curves for HEC-1-A and RL95-2 cells resulting when a bovine serum albumin (BSA)-coated microbead (BSA) (**A**, **B**) or a JAR-coated microbead (JAR) (**C**, **D**) was retracted after periods of 1–40 min of contact. The horizontal axis shows the vertical movement of the cantilever; the vertical axis shows the force acting on the microbead. Note force rupture events when a JAR-coated microbead was retracted from RL95-2 cells (**D**). For interaction code see Figure 3.

atomic force microscope, interaction forces between trophoblast and uterine epithelium were examined *in vitro*. In our model cell culture system, it was possible to define features of adhesive interactions and their time-dependent development that appear to be correlated with cell behaviour, i.e. the ability of uterine epithelial RL95-2 (RL cells) and the inability of uterine epithelial HEC-1-A (HEC cells) to attach strongly to trophoblast-type cells via their apical (free) cell poles. These findings open new ways to explain mechanisms behind the phenomenon that the apical (free) membrane surface of epithelial RL cells is somehow predisposed for trophoblast adhesion, in contrast to other cells, as discussed below. With

regard to a general knowledge of cell adhesion, our data may have relevance for a basic description of the kinetics of binding and of binding strength as well as for methods for studying cell-to-cell interactions (e.g. Mege *et al.*, 1986; Tha and Goldsmith, 1986; Tha *et al.*, 1986; Evans *et al.*, 1991, 1995; Tees *et al.*, 1993).

Forces measured during the approach part of the experiment, i.e. before the onset of adhesive interactions, were repulsive. This was true no matter whether the probe (a microbead mounted on a cantilever) was naked (coated with BSA) or covered with JAR cells. Soft and hard repulsion was observed. While a long-ranged soft repulsion might be due to peripheral

structures of the cell (e.g. glycocalyx, microvilli, and micro-ridges), the subsequently recorded hard repulsion is probably dependent on structures that are located more deeply inside the cytoplasm (e.g. the relative rigidity caused by cytoskeletal elements). Associated with their rough surface (Thie *et al.*, 1995), HEC cells showed a long range of soft repulsion in combination with a continuous transition to the hard repulsion regime at relatively high indentation forces. In contrast, the smooth-surfaced RL cells (Thie *et al.*, 1995) showed lower values of indentation force at the beginning of hard repulsion after an abrupt transition. HEC cells have previously been shown to possess a thicker glycocalyx than RL cells (Thie and Denker, 1997).

Interestingly, only BSA-coated microbeads showed immediate adhesion while JAR-coated microbeads did not. After prolonged contact times of JAR-coated microbeads with the uterine monolayers, however, the separation curves changed and became indicative of adhesion events. Adhesion increased progressively. Increase in adhesion might be due to substitution of proteins during contact (Vroman effect: Scott, 1991) or progressive flattening of cell surfaces and increase of contact area. As the contact zone has not yet been investigated, it is not known whether JAR cells attach to the entire apical surface of endometrial cells or to localised regions of this surface. Whatever the reason, the increase in adhesive forces stopped and reached saturation for contact periods of 20 and 40 min. Saturation of adhesive forces might be due to reaching a steady state of substitution processes and/or narrowing of contact sites. Profiles of separation curves of BSA-microbeads in contact with HEC/RL cells as well as of JAR-microbeads in contact with HEC cells showed marked similarities and may be interpreted as representing the stretching of cells for a short distance (low width of the adhesion maximum). The decreasing adhesion shoulder in the long distance range might reflect the formation of tethers (Hochmuth *et al.*, 1996) which are pulled out of the apical membrane. More interestingly, the shape of the JAR/RL separation curves as seen after prolonged contact times clearly indicates a different kind of interaction. The fact that, at first, repeated rupture events were observed in the range of 1–3 nN with a distance between 7–15  $\mu\text{m}$  and, thereafter, a final rupture event at a distance of up to 45  $\mu\text{m}$  points to quite a different mechanism, i.e. the breaking of comparably strong cell-to-cell bonds. This assumption is supported by the finding that in some cases after the experiment the RL monolayer was visibly damaged, a phenomenon that was not observed in our experiments with HEC cells (data not shown). In previous experiments using a centrifugal force-based adhesion assay (John *et al.*, 1993), it was shown that RL cells readily allowed JAR-cell spheroids to attach firmly and even to insinuate between them, whereas HEC cells did not. We conclude from this that the pattern of plateau formation with minor peaks followed by a final rupture event, as seen in the RL-JAR cell combination, is indicative of firm membrane adhesion.

The cell adhesion molecules that actually mediate trophoblast adhesion to the apical (free) surface of uterine epithelial cells are still unknown. Various types of molecules have been proposed to play a role in this process (for review, see Lopata,

1996). Among them, integrins are discussed as molecules that may mediate cell-to-cell binding between uterine epithelium and trophoblast (Lessey *et al.*, 1992, 1994; Albers *et al.*, 1995; Bronson and Fusi, 1996). Indeed, in RL cells, integrins, e.g.  $\alpha 6$ -,  $\beta 1$ - and  $\beta 4$ -integrin subunits, are expressed along the entire plasma membrane including the apical (free) cell surface (Thie *et al.*, 1995). In HEC cells, however, the same integrins are absent from the apical cell pole (Thie *et al.*, 1995). Successful binding between uterine cells and the trophoblast may require not only that appropriate adhesion molecules are present but also that these are accessible to their ligand. Thus, the relative ability of cell surface molecules to gain access to their targets might be related to a low level of sterical hindrance by the glycocalyx and, for example, to the removal of a cell surface-associated mucin, MUC-1 (Aplin *et al.*, 1994). In the present series of experiments, the approach of JAR cells seemed to be only slightly easier to RL than to HEC cells. It will have to be determined in subsequent investigations whether this slight difference is related to the known differences of the glycocalyx (Thie and Denker, 1997), and if it is of any significance for the different behaviour of RL and HEC cells in the centrifugal force-based attachment assay (John *et al.*, 1993). Also the free surface of RL cells is dome-like and largely free of microvilli while the apical surface of HEC cells is covered with microvilli; a smooth surface (e.g. RL cells) should be more accessible than a rough surface (e.g. HEC cells). Although not yet investigated, the tightness of apposition of confronted RL cells and JAR cells might modulate the quality of cell-to-cell adhesion. A further point that merits study in subsequent investigations is that cell surfaces exposed to serum-containing media will rapidly become coated by a layer of adsorbed molecules, which might act as bridging ligands.

Our data suggest that adhesion of trophoblast to uterine epithelium might be a relatively slow process, possibly including signal transduction cascades and sequential steps of bond formation. This contact may precede trophoblast migration and early placentation (Bischof and Campana, 1996; Burrows *et al.*, 1996). There is evidence suggesting that the initiation of the adhesion process requires a certain degree of pressure exerted between the surfaces of trophoblast (in the case of our model: JAR cells) and uterine epithelium, *in vivo* and *in vitro*. *In vivo*, myometrial contraction and/or endometrial oedema might secure tight apposition (Enders, 1976, 1993; Mitchell *et al.*, 1987). *In vitro*, it was found essential to secure the tight packing of rabbit blastocysts and endometrial fragments in order to achieve attachment (Hohn and Denker, 1990). Interestingly, cultured human blastocysts are described as attaching to endometrial epithelial cells by just resting on them (Lindenberg *et al.*, 1986, 1989). In the present experiments, however, the initiation of adhesion seemed to depend on a preparative phase of pressing the probe (cantilever with JAR-coated microbead) against the uterine monolayer. We have previously shown that the mechanical stimulation of RL cells via apical membrane-bound integrins (using paramagnetic beads and a magnetic force drag device) can elicit intracellular calcium waves which may be one aspect of such mechanical signalling. In that case, stimulation of integrins provoked a

calcium response in RL cells 50–150 s ( $\alpha 6$ -integrin subunits) and 200–300 s ( $\beta 1$ -integrin subunits) after starting stimulation and it was dependent on an intact cytoskeleton (Thie *et al.*, 1997). So far, no further details are known about this signalling pathway in RL cells and how the signal is networked. Nevertheless, it is likely to include the activation of kinases, small molecular mass guanosine triphosphatases, phospholipid mediators and/or changes in cytoskeletal linkages.

In conclusion, the data presented here are consistent with the concept that uterine epithelial cells in the receptive state possess a reorganized epithelial phenotype, i.e. a non-polarized architecture and, thus, a luminal plasma membrane equipped with appropriate adhesion molecules; if the trophoblast is positioned on to the surface for sufficient periods of time, a cascade of events can be initiated that leads to the formation of strong adhesion. Moreover, the modified atomic force microscope technique introduced in the present communication promises to offer a novel tool that can allow the investigation of details of the underlying mechanisms and molecules playing a role in the cell-to-cell interactions in implantation.

### Acknowledgements

The skilful technical assistance of Birgit Maranca-Nowak, Ulrike Trottenberg, Dorothea Schünke, Marion Nissen, Saurbek Kuschhabiew, and Dave Kittel is gratefully acknowledged. We would like to thank Gebhard Reiss for helpful comments. This work was supported by the Deutsche Forschungsgemeinschaft. R.R. was supported by funds from the Mildred Scheel Stiftung to H.-P. Hohn and H.-W.D.

### References

- Albers, A., Thie, M., Hohn, H.-P. *et al.* (1995) Differential expression and localization of integrins and CD44 in the membrane domains of human uterine epithelial cells during the menstrual cycle. *Acta Anat.*, **153**, 12–19.
- Aplin, J.D., Seif, M.W., Graham, R.A. *et al.* (1994) The endometrial cell surface and implantation: expression of the polymorphic mucin MUC-1 and adhesion molecules during the endometrial cycle. *Ann. N.Y. Acad. Sci.*, **734**, 103–121.
- Bentin-Ley, U., Pedersen, B., Lindenberg, S. *et al.* (1994) Isolation and culture of human endometrial cells in a three-dimensional culture system. *J. Reprod. Fert.*, **101**, 327–332.
- Binnig, G., Quate, C.F. and Gerber, C. (1986) Atomic force microscope. *Phys. Rev. Lett.*, **56**, 930.
- Bischof, P. and Campana, A. (1995) A model for implantation of the human blastocyst and early placentation. *Hum. Reprod. Update*, **2**, 262–270.
- Bronson, R.A. and Fusi, F.M. (1996) Integrins and human reproduction. *Mol. Hum. Reprod.*, **2**, 153–168.
- Burrows, T.D., King, A. and Loke, Y.W. (1996) Trophoblast migration during human placental implantation. *Hum. Reprod. Update*, **2**, 307–321.
- Carson, D.D., Tang, J.P., Julian, J. *et al.* (1988) Vectorial secretion of proteoglycans by polarized rat uterine epithelial cells. *J. Cell Biol.*, **107**, 2425–2435.
- Cross, R.H.M. (1989) A reliable epoxy resin mixture and its application in routine biological transmission electron microscopy. *Micron Microsc. Acta*, **20**, 1–7.
- Dammer, U., Hegner, M., Anselmetti, D. *et al.* (1995) Specific antigen/antibody interactions observed by atomic force microscopy. *Biophys. J.*, **70**, 2437–2441.
- Denker, H.-W. (1993) Implantation: a cell biological paradox. *J. Exp. Zool.*, **266**, 541–558.
- Denker, H.-W. (1994) Endometrial receptivity: cell biological aspects of an unusual epithelium. *Ann. Anat.*, **176**, 53–60.
- Enders, A.C. (1976) Anatomical aspects of implantation. *J. Reprod. Fert.*, Suppl. **25**, 1–15.
- Enders, A.C. (1993) Overview of the morphology of implantation in primates. In Wolf D.P. (ed.), *In vitro Fertilization and Embryo Transfer in Primates*. Serono Symposia, USA. Springer-Verlag, New York, pp. 145–157.
- Evans, E., Berk, D. and Leung, A. (1991) Detachment of agglutinin bonded red blood cells I. Forces to rupture molecular point attachments. *Biophys. J.*, **59**, 838–848.
- Evans, E., Richtie, K. and Merkel, R. (1995) Sensitive force technique to probe molecular adhesion and structural linkages at biological interfaces. *Biophys. J.*, **68**, 2580–2587.
- Florin, E.-L., Moy, V.T. and Gaub, H.E. (1994) Adhesive forces between individual ligand-receptor pairs. *Science*, **264**, 415–417.
- Glasser, S.R., Julian, J., Decker, G.L. *et al.* (1988) Development of morphological and functional polarity in primary cultures of immature rat uterine epithelial cells. *J. Cell Biol.*, **107**, 2409–2423.
- Hertz, H. (1881) Über den Kontakt elastischer Körper. *J. Reine Angew. Mathematik*, **92**, 156.
- Hinterdorfer, P., Baumgartner, W., Gruber, H.J. *et al.* (1996) Detection and localization of individual antibody-antigen recognition events by atomic force microscopy. *Proc. Natl. Acad. Sci. USA*, **93**, 3477–3481.
- Hochmuth, R.M., Shao, J.-Y., Dai, J. *et al.* (1996) Deformation and flow of membrane into tethers extracted from neuronal growth cones. *Biophys. J.*, **70**, 358–369.
- Hohn, H.-P. and Denker, H.-W. (1990) A three-dimensional organ culture model for the study of implantation of rabbit blastocyst *in vitro*. In Denker, H.-W. and Aplin, J.D. (eds), *Trophoblast Invasion and Endometrial Receptivity. Novel Aspects of the Cell Biology of Embryo Implantation*. Trophoblast Research Vol. 4. Plenum Medical Book Comp., New York, London. pp. 71–95.
- John, N., Linke, M. and Denker, H.-W. (1993) Quantitation of human choriocarcinoma spheroid attachment to uterine epithelial cell monolayers. *In vitro Cell. Dev. Biol.*, **29A**, 461–468.
- Kuramoto, H., Tamura, S. and Notake, Y. (1972) Establishment of a cell line of human endometrial adenocarcinoma *in vitro*. *Am. J. Obstet. Gynecol.*, **114**, 1012–1019.
- Lessey, B.A., Castelbaum, A.J., Buck, C.A. *et al.* (1994) Further characterization of endometrial integrins during the menstrual cycle and in pregnancy. *Fertil. Steril.*, **62**, 497–506.
- Lessey, B.A., Damjanovich, L., Coutifaris, C. *et al.* (1992) Integrin adhesion molecules in the human endometrium. *J. Clin. Invest.*, **90**, 188–195.
- Lindenberg, S., Hyttel, P., Lenz, S. *et al.* (1986) Ultrastructure of the early human implantation *in vitro*. *Hum. Reprod.*, **1**, 533–538.
- Lindenberg, S., Hyttel, P., Sjogren, A. *et al.* (1989) A comparative study of attachment of human, bovine and mouse blastocysts to uterine epithelial monolayer. *Hum. Reprod.*, **4**, 446–456.
- Lopata, A. (1996) Blastocyst-endometrial interaction: an appraisal of some old and new ideas. *Mol. Hum. Reprod.*, **2**, 519–525.
- Ludwig, M., Dettmann, W. and Gaub, H.E. (1997) AFM imaging contrast based on molecular recognition. *Biophys. J.*, **72**, 445–448.
- Mege, J.L., Capo, C., Benoliel, A.M. *et al.* (1986) Determination of binding strength and kinetics of binding initiation. A model study made on the adhesive properties of P388D1 macrophage-like cells. *Cell Biophysics*, **8**, 141–160.
- Mitchell, J.A., Driessen, G., Scheidt, H. *et al.* (1987) Changes in intraconceptus pressure in the rabbit during days 7–10 of pregnancy. *Biol. Reprod.*, **36**, 669–675.
- Pattillo, R.A., Ruckert, A., Hussa, R. *et al.* (1971) The JAR cell line – continuous human multihormone production and controls. *In Vitro*, **6**, 398.
- Psychoyos, A. (1995) Nidation window: from basic to clinic. In Dey, S.K. (ed.), *Molecular and Cellular Aspects of Peri-implantation Processes*. Springer-Verlag, New York. pp. 1–14.
- Raboudi, N., Julian, J., Rohde, L.H. *et al.* (1992) Identification of cell surface heparin/heparan sulfate binding proteins of a human uterine epithelial cell line (RL95). *J. Biol. Chem.*, **267**, 11930–11939.
- Radmacher, M., Tillmann, R.W., Fritz, M. *et al.* (1992) From molecules to cells – imaging soft samples with the AFM. *Science*, **257**, 1900–1905.
- Radmacher, M., Fritz, M. and Hansma, P.K. (1995) Imaging soft samples with the atomic force microscope: gelatin in water and propanol. *Biophys. J.*, **69**, 264–270.
- Rief, M., Gautel, M., Oesterhelt, F. *et al.* (1997) Reversible unfolding of individual titin Ig-domains by AFM. *Science*, **276**, 1109–1112.
- Rogers, P.A. (1995) Current studies on human implantation: a brief overview. *Reprod. Fert. Dev.*, **7**, 1395–1399.
- Rohde, L.H. and Carson, D.D. (1993) Heparin-like glycosaminoglycans participate in binding of a human trophoblastic cell line (JAR) to a human uterine epithelial cell line (RL95). *J. Cell. Physiol.*, **155**, 185–196.

- Rohde, L.H., Julian, J., Babaknia, A. *et al.* (1996) Cell surface expression of HIP, a novel heparin/heparan sulfate-binding protein, of human uterine epithelial cells and cell lines. *J. Biol. Chem.*, **271**, 11824–11830.
- Rugar, D. and Hansma, P.K. (1990) Atomic force microscopy. *Physics Today*, **43**, 23–30.
- Scott, C.F. (1991) Mechanism of the participation of the contact system in the Vroman effect. *J. Biomat. Sci.*, **2**, 173–181.
- Tabibzadeh, S. and Babaknia, A. (1995) The signals and molecular pathways involved in implantation, a symbiotic interaction between blastocyst and endometrium involving adhesion and tissue invasion. *Mol. Hum. Reprod.*, **1**, 1579–1602.
- Tees, D.F.J., Coenen, O. and Goldsmith, H.L. (1993) Interaction forces between red cells agglutinated by antibody. IV. Time and force dependency of break-up. *Biophys. J.*, **65**, 1318–1334.
- Tha, S.P. and Goldsmith, H.L. (1986) Interaction forces between red cells agglutinated by antibody. I. Theoretical. *Biophys. J.*, **50**, 1109–1116.
- Tha, S.P., Shuster, J. and Goldsmith, H.L. (1986) Interaction forces between red cells agglutinated by antibody. II. Measurement of hydrodynamic force of break-up. *Biophys. J.*, **50**, 1117–1126.
- Thie, M. and Denker, H.-W. (1997) Endometrial receptivity for trophoblast attachment: model studies using cell lines. In Motta, M. (ed.), *Microscopy of Reproduction and Development. A Dynamic Approach*. P. Antonio Delfino Editore S.r.l., Roma, pp. 241–249.
- Thie, M., Harrach-Ruprecht, B., Sauer, H. *et al.* (1995) Cell adhesion to the apical pole of epithelium: a function of cell polarity. *Eur. J. Cell Biol.*, **66**, 180–191.
- Thie, M., Fuchs, P. and Denker, H.-W. (1996a) Epithelial cell polarity and embryo implantation in mammals. *Int. J. Dev. Biol.*, **40**, 389–393.
- Thie, M., Fuchs, P., Butz, S. *et al.* (1996b) Adhesiveness of the apical surface of uterine epithelial cells: the role of junctional complex integrity. *Eur. J. Cell Biol.*, **70**, 221–232.
- Thie, M., Herter, P., Pommerenke, H. *et al.* (1997) Adhesiveness of the free surface of a human endometrial monolayer for trophoblast as related to actin cytoskeleton. *Mol. Hum. Reprod.*, **3**, 275–283.
- Way, D.L., Grosso, D.S., Davis, J.R. *et al.* (1983) Characterization of a new human endometrial carcinoma (RL95-2) established in tissue culture. *In Vitro*, **19**, 147–158.

Received on February 12, 1998; accepted on August 12, 1998